

Visualization of Particle Flux in the Human Body on the Surface of Mars

PREMKUMAR B. SAGANTI^{1, 2*}, FRANCIS A. CUCINOTTA²,
JOHN W. WILSON³ and WALTER SCHIMMERLING³

Mars / Radiation / Human body / Visualization / GCR

For a given galactic cosmic ray (GCR) environment, information on the particle flux of protons, alpha particles, and heavy ions, that varies with respect to the topographical altitude on the Martian surface, are needed for planning exploration missions to Mars. The Mars Global Surveyor (MGS) mission with its Mars Orbiter Laser Altimeter (MOLA) instrument has been providing precise topographical surface map of the Mars. With this topographical data, the particle flux at the Martian surface level through the CO₂ atmospheric shielding for solar minimum and solar maximum conditions are calculated. These particle flux calculations are then transported first through an anticipated shielding of a conceptual shelter with several water equivalent shield values (up to 50 g/cm² of water in steps of 5 g/cm²) considered to represent a surface habitat, and then into the human body. Model calculations are accomplished utilizing the HZETRN, QMSFRG, and SUM-MARS codes. Particle flux calculations for 12 different locations in the human body were considered from skin depth to the internal organs including the blood-forming organs (BFO). Visualization of particle flux in the human body at different altitudes on the Martian surface behind a known shielding is anticipated to provide guidance for assessing radiation environment risk on the Martian surface for future human missions.

INTRODUCTION

If the later part of the 20th century is considered to be a *small step* based on the human landing that occurred on the Moon, indeed, it will be a *giant leap* when the humans reach Mars in the early part of the 21st century. In planning human exploration missions, NASA and other space agencies involved in these endeavors will place a high priority on the health and safety of astronauts¹⁾. A major area of concern is the possible detrimental effect on health, including cancer, a broad-range of degenerative tissue diseases including damage to the central nervous system, cataracts, and hered-

itary risks, caused by exposure to galactic cosmic rays (GCR). The GCR contain high-energy protons and highly ionizing heavy ions that have large penetration power in shielding and tissue and are unlike any radiation to which humans are exposed on Earth. It is not possible to completely shield the GCR environment with practical amounts of radiation shielding because of their ranges in materials and the production of secondary particles including neutrons as the GCR penetrate materials²⁾.

In this report, we present the model calculations and predictions of the particle flux of protons, alpha particles, and heavy ions on the Martian surface at various solar cycle scenarios. As a particle passes through tissues, cells, or DNA, ionization events on biomolecules occur leading to the production of secondary electrons. Close to an ion track, particles directly excite biomolecules. Lower energy electrons produced in these events deposit a large amount of energy, however are confined to a small radial region about the ion track in the so called track core. Higher-energy electrons ejected by the ion are termed as γ -rays and impart energy in other areas of the cell or even in adjacent cells³⁾. The term *track structure* refers to the description of the spatial distri-

*Corresponding author: Phone: +1 281-483-5168

Fax: +1 281-483-2696

E-mail: premkumar.saganti1@jsc.nasa.gov

¹Lockheed Martin Space Operations, NASA-JSC, Houston, TX-77058

²NASA Johnson Space Center, Houston, TX-77058

³NASA Langley Research Center, Hampton, VA-23681

⁴NASA Head Quarters, Washington, DC-20546

bution of energy deposition events at the biomolecular level. Because the uncertainties in defining the dose equivalent for the GCR are large⁴, alternate quantities to discuss risks for exploration missions are needed. Here we consider one basic property, the number of particle traversals or hits per cell. We note that other quantities will be discussed elsewhere.

In our present model calculations, we consider detailed calculations of the particle flux and organ dose equivalent values at several locations on the surface of Mars with the inclusion of static CO₂ atmospheric shielding model based on the MOLA data⁵. Particle fluxes are presented in terms of the probable number of cell hits by protons, alpha particles, and heavy ions ($3 \leq Z \leq 10$, $11 \leq Z \leq 20$, $21 \leq Z \leq 28$) in order to provide insights into the risks on the Mars surface from different GCR components. These calculations and model predictions are expected to provide requirements for radiation shield development and also influence the ongoing radiobiology research investigations to assess future human missions to Mars.

MATERIALS AND METHODS

GCR Spectra

Using the HZETRN transport code, GCR spectra for several solar maximum and solar minimum scenarios were generated. Following Badhwar and O'Neill model⁶ the solar effects on the GCR are described in terms of the solar modulation parameter, Φ , with the results shown here are for the current solar maximum ($\Phi = 1075$ MV) (anticipated for the year, 2002) and near solar minimum ($\Phi = 428$ MV). The contribution from the Solar Particle Events (SPE) is not included in the present calculations. Calculations that include spectral data from past SPE will be presented elsewhere.

Particle Flux

Making use of the HZETRN transport code⁷ and the QMSFRG nuclear interaction model⁸ the particle flux, $\phi_j(x, E)$, of ion, j with energy, E and depth, x is obtained from

$$\Omega \cdot \nabla \phi_j(x, \Omega, E) = \sum_k \int \sigma_{jk}(\Omega, \Omega', E, E') \phi_k(x, \Omega', E') d\Omega' dE' - \sigma_j(E) \phi_j(x, \Omega, E)$$

The methods of Wilson et al.,⁷ for GCR transport is to use the straight-ahead and continuous slowing down approximation to solve the above equation for charged ions and to include angular effects for neutrons.

Martian CO₂ Model

For two different density models (16 and 22 g/cm³), spherically distributed CO₂ atmosphere was considered⁹. In each atmospheric model, variation of CO₂ density with respect to altitude was also considered are available from ref.⁹. The variations in the CO₂ density due to sporadic temperature changes is not completely know and hence these changes are not incorporated in the current model. The resultant shielding offered by the CO₂ atmosphere at a given altitude location is calculated for a set of 512 rays using the relation

$$s(z, \theta) = \sqrt{(R+h)^2 \cos^2(\theta) + [2R(z-h) + z^2 - h^2]} - (R+h) \cos(\theta)$$

Where, h is the altitude above the mean surface, s being the distance along the slant path with zenith angle, θ , (calculated between 0 and 90° with 10° increments) and z is the vertical height of the atmosphere above the identified location.

Visualization in the Human Body

Utilizing the SUM-MARS code¹⁰, the intrinsic shield values offered by the human body for 12 different anatomical locations were calculated based on the CAM (Computerized Anatomical Male) shielding description. Then the flux of the particles (neutrons, alpha, low, medium, and heavy ions) that were generated for various solar cycle scenarios was transported through the human body shielding. Visualization of the organ dose-equivalent values (cSv/yr), along with probable particle-hits by protons and heavy-ions (particle-hits/cell/yr) are presented in the human body on the Martian mean surface. The cell dimension considered was 100 μm^2 . Visualization of the interactive human model was accomplished using the SRHP (Space Radiation Health Project at NASA Johnson Space Center)¹¹ developed VIZ-MARS routines¹² utilizing the MATLAB-5.1 resources¹³. These human body visualization techniques are based on our earlier work reported in the year 2001¹⁴.

Description of the CAM Model

Human body shield values are calculated utilizing the CAM model originally developed by Paul Kase in the 1970s¹⁵. The CAM model consists of about 1500 quadratic surfaces that result in about 2500 closed volumes¹⁶. Current resolution of the model is about 0.1 inch and is represented within 5% of organ size and body weight. Anatomical composition is modeled for 11 different tissue types. Typically, the CAM model represents a 50th percentile U. S. Air Force cohort of about 5' 9.25" (~ 176 cm) height and 155 lbs (70 kg) weight. In our current visualization, we have used a 19"

$\times 19'' \times 71''$ ($\sim 48 \times 48 \times 180 \text{ cm}^3$) 3D-lattice to represent our calculated data. Though at this time, the CAF (computerized anatomical female) model is available at the NASA Johnson Space Center, we have not used it for our calculations¹⁷⁾. We intend to present our results for the CAF model in future publications.

RESULTS AND DISCUSSION

Projections of the particle-hits per cell on the Mars surface are estimated for 12 different organ depths in a human body behind a given conceptual vehicle with known water equivalent shielding. Radiation elemental fluxes on the Martian surface at 12 different anatomical locations inside of the human body for a given GCR environment are calculated (Table-1). Visualization of the dose-equivalent values and particle-hits per cell on the Martian surface are presented to illustrate the range of variation inside of the human body at the mean surface level on Mars (Fig. 1-3). Though not included in this report, variations of the particle flux distribution as a function of entire Martian topography above and below the mean surface were also calculated and presented by Cucinotta et al., in this volume¹⁸⁾. The human body self-shielding from the outermost point level to the innermost organ level indicate a particle flux reduction of \sim

2% for the protons ($Z=1$) and $\sim 35\%$ for the heavy ions ($Z \geq 2$). The addition of water shielding for solar minimum condition indicates significant reduction for heavy ion flux, moderate reduction for alpha particles, and little or no reduction for neutron and protons. With a 40 g/cm^2 water shield at the mean surface level, the particle flux at skin level is noted as follows: heavy ion flux decreased by a factor of 30, medium ions by a factor of 12, light ions by a factor of 4, alpha particles by a factor of 3, the flux of protons essentially remained unchanged.

The models used here for the GCR particle flux predictions show good agreement with the cruise-phase (April-August, 2001) and orbital phase (April 2002 – present) data of the Martian Radiation Environment Experiment (MARIE) instrument of the 2001 Mars Odyssey mission as will be described elsewhere¹⁹⁾. Also, in this report, we have not included any detailed calculations of the *albedo* neutrons produced in interactions with the Mars atmosphere or surface. Such data will be needed to make a complete estimate of the exposures to be encountered on Mars. Quantifying the radiation risk uncertainty⁴⁾ and mitigating the radiation risk on the Martian surface has been a priority for future manned missions to the Mars and for radiobiological investigations of the current era.

Table 1. Model calculations of probable particle-hits per cell at skin depth in one year near solar maximum ($\Phi = 1075 \text{ MV}$). Calculations are for 12 different organ locations in a human body at the mean surface level on Mars

Human Body on the Martian Surface (Mean Altitude)	Particle-Hits / Cell / Year near solar maximum					
	Protons $Z = 1$	Alpha Particles $Z = 2$	Light Ions $3 \leq Z \leq 10$	Medium Ions $11 \leq Z \leq 20$	Heavy Ions $21 \leq Z \leq 28$	All ($Z \geq 2$)
1 Skin	42.7	1.46	0.08	0.0067	0.0011	1.55
2 Eye	42.8	1.52	0.08	0.0069	0.0011	1.61
3 Blood Forming Organs (BFO)	42.6	1.32	0.06	0.0047	0.0006	1.39
4 Stomach	42.6	1.23	0.06	0.0038	0.0005	1.29
5 Colon	42.6	1.32	0.06	0.0046	0.0006	1.39
6 Liver	42.6	1.25	0.06	0.0041	0.0005	1.31
7 Lungs	42.5	1.29	0.06	0.0044	0.0006	1.36
8 Bladder	42.4	1.21	0.06	0.0037	0.0004	1.27
9 Thyroid	42.6	1.35	0.07	0.0050	0.0007	1.42
10 Esophagus	42.5	1.28	0.06	0.0043	0.0006	1.34
11 Gonads	42.4	1.31	0.06	0.0048	0.0007	1.37
12 POINT	43.2	1.84	0.10	0.0098	0.0017	1.95

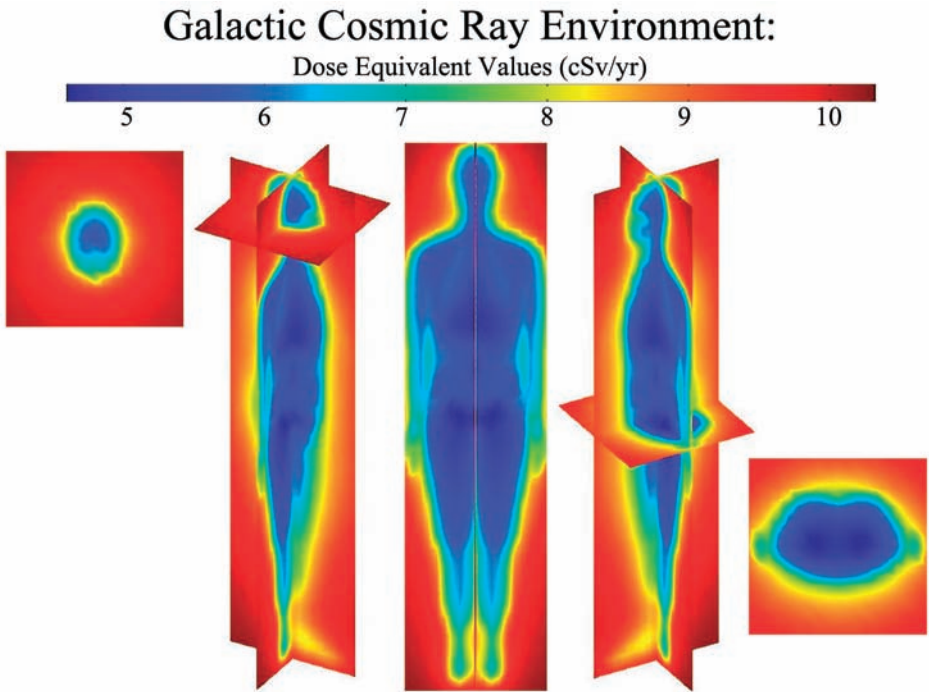


Fig. 1. Model predictions of the dose-equivalent values (cSv/yr) from the GCR at the mean surface level on the Martian surface. Calculations are shown at skin depth for a solar maximum scenario ($\Phi = 1075$ MV).

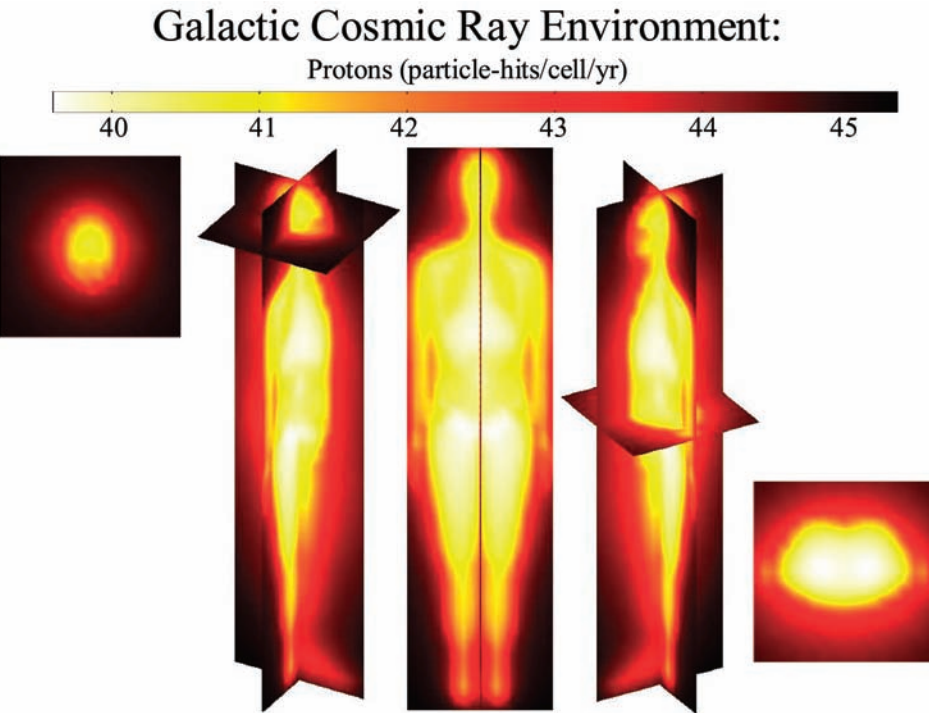


Fig. 2. Model predictions of proton flux (particle-hits/cell/yr) from the GCR contribution at the mean surface level on the Martian surface. Calculations are shown at skin depth for a solar maximum scenario ($\Phi = 1075$ MV).

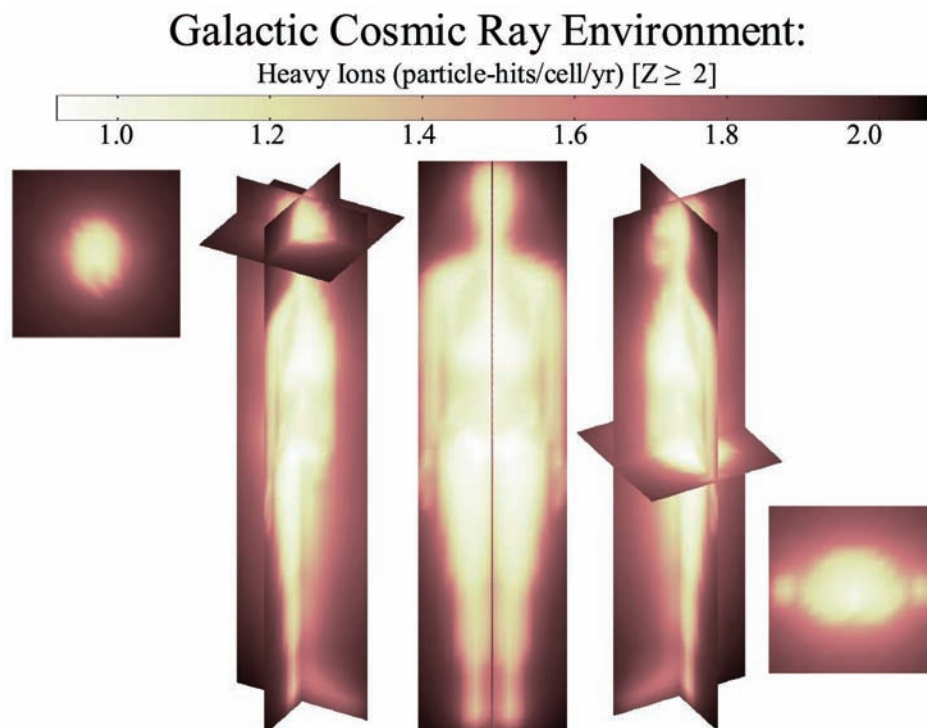


Fig. 3. Model predictions of all ions ($Z \geq 2$ shown as particle-hits/cell/yr) from the GCR contribution at the mean surface level on the Martian surface. Calculations are shown at skin depth for a solar maximum scenario ($\Phi = 1075$ MV).

REFERENCES

1. National Academy of Sciences (2002) Safe on Mars: Precursor Measurements Necessary to Support Human Operations on the Martian Surface, National Academy Press, Washington, D.C.
2. Wilson, J. W., Miller, J., Konradi, A. and Cucinotta, F. C. (1997) Shielding Strategies for Human Space Exploration, NASA CP – 3360.
3. Cucinotta, F. A., Nikjoo, H. and Goodhead, D. T. (1998) The Effects of Delta Rays on The Number of Particle-Track Traversals per Cell in Laboratory and Space Exposures, *Radiat. Res.* **150**: 115–119.
4. Cucinotta, F. A., Schimmerling, W., Wilson, J. W., Peterson, L. E., Badhwar, G. D., Saganti, P. B. and Dicello, J. F. (2001) Space Radiation Cancer Risks and Uncertainties for Mars Missions, *Radiat. Res.* **156**: 682–688.
5. Smith, D. E., Zuber, M. T., Solomon, S. C., Philips, R. J., Head, J. W., Garvin, J. B., *et al.* (1999) The Global Topography of Mars and Implications for Surface Evolution, *Science* **284**: 1495–1503.
6. Badhwar, G. D. and O'Neill, P. M. (1996) Galactic cosmic radiation model and its applications, *Adv. Space Res.* **17**: 7–17.
7. Wilson, J. W., Badavi, F. F., Cucinotta, F. A., Shinn, J. L. and Badhwar, G. D. (1995) HZETRN: description of a free-space ion and nucleon transport and shielding computer program. Springfield, VA: National Technical Information Service: NASA TP 3495
8. Cucinotta, F. A., Wilson, J. W., Shinn, J. L. and Tripathi, R. K. (1998) Assessment and Requirements of Nuclear Reaction Data Bases for GCR Transport in the Atmosphere and Structures. *Adv. Space. Res.* **21**: 1753–1762.
9. Simonsen, L. C., Wilson, J. W., Kim, M. H. and Cucinotta, F. A. (2000) Radiation Exposure for Human Mars Exploration, *Health Phys.*, **79** (5): 515–525.
10. Cucinotta, F. A. (1999) SUMCAM: Summation and average dose distribution for the CAMERA shield data files. Unpublished work, Space Radiation Health Project, NASA Johnson Space Center, November.
11. NASA Johnson Space Center, Space Radiation Health Project: SRHP Website (2002) <http://srhp.jsc.nasa.gov/>
12. Saganti, P. B., Cucinotta, F. A. and Zapp, E. N. (2000) Visualization and Animation of 3D-Lattice data utilizing the MATLAB-5 software. Un published work, Space Radiation Health Project, NASA Johnson Space Center.
13. The MathWorks, Inc., Natick, MA-01760, USA; MATLAB-5 Software, 1999–2000
14. Saganti, P. B., Zapp, E. N., Wilson, J. W. and Cucinotta, F. A. (2001) Visual Assessment of the Radiation Distribution in the ISS Lab Module: Visualization in the Human Body, *Physica Medica* **XVII** (1): 106–112.
15. Kase, P. G. (1970) Computerized Anatomical Model Man,

- Kirtland Air Force Base, New Mexico, Technical Report No. AFWL-TR-**69-161**.
16. Billings, M. P., Yucker, W. R. and Heckman, B. R. (1973) Body Shelf shielding Data Analysis, McDonnell Douglas Astronautics Company-West, MDC-**G4131**.
 17. Yucker, W. R., Huston, S. L. and Reck, R. J. (1990) Computerized Anatomical Female, McDonnell Douglas Space Systems Company, MDC-**H6107**.
 18. Cucinotta, F. A., Saganti, P. B., Wilson, J. W. and Simonsen, L. C. (2002) Model Predictions and Visualization of the Particle Flux on the Surface of Mars. *J. Radiat. Res.* **43 Suppl.**: S35–S39.
 19. NASA Johnson Space Center, Martian Radiation Environment Experiment: MARIE Website (2002) <http://marie.jsc.nasa.gov/>

Received on June 10, 2002

Revision on August 26, 2002

Accepted on November 1, 2002